AIAA JOURNAL
Vol. 38, No. 7, July 2000

Self-Similarity of Hydroxyl-Concentration Temporal Statistics in Turbulent Nonpremixed Jet Flames

Michael W. Renfro,* Jay P. Gore,† Galen B. King,‡ and Normand M. Laurendeau§
Purdue University, West Lafayette, Indiana 47907-1288

Temporal statistics for hydroxyl concentrations in turbulent nonpremixed hydrogen/argon flames have recently been reported in the form of power spectral densities for a range of Reynolds numbers (2.8×10^3–1.7×10^4) and axial locations ($x/D = 1$–20). In the present investigation these data are examined further, and the two-time statistics are shown to collapse when scaled by the measured integral timescale. The resulting autocorrelation function is shown to be closely approximated by an exponential decay, as previously reported for mixture fraction. The measured integral timescales vary with Reynolds number and position within the reacting jet in accordance with a simple similarity scaling. The implications of this unexpected statistical similarity are examined with respect to the simulation of scalar fluctuations in turbulent nonpremixed flames.

Introduction

SELF-SIMILARITY in velocity and scalar cross-stream profiles for nonreacting turbulent jets was established many years ago. These profiles provide a useful representation of mean velocity and scalar fields because, significantly downstream of the jet exit, the cross-stream variations are found to depend only on a single length scale and a single velocity scale. The appropriate scaling parameters, such as the centerline velocity and jet width, display characteristic decay and growth rates that are consistent with fundamental dimensional relationships. The existence of self-similarity for higher-order statistics, such as the variance, has also been observed sufficiently downstream of the jet exit.[1,2] However, these profiles may still depend on some details of the jet.[1]

Time-series measurements of velocity and mixture fraction in nonreacting jets have also displayed self-similar behavior in terms of the power spectral density (PSD) and the autocorrelation function.[2,3] In particular, these two-time statistics appear to collapse onto a single curve when normalized by a single timescale, such as the integral timescale. However, as the jet Reynolds number increases, the energy bearing and dissipative scales become further separated.[4] Thus, a single timescale cannot truly be adequate in describing fluctuations at all frequencies, and the observed collapse of two-time statistics when normalizing by the integral time scale is actually limited to fluctuations sufficiently above the Kolmogorov frequency. Alternatively, a second parameter, such as another timescale or the Reynolds number, can be used to collapse the full spectrum.[5]

The existence of self-similarity for scalars in reacting flows is less clear owing both to the effects of source terms and to the interaction between heat release and turbulence. Kounalakis et al.[6] found self-similar autocorrelation functions for mixture fraction and path-integrated radiation in hydrogen jet flames, but their results should not hold for the mean concentration profiles of those reacting scalars that depend strongly on detailed chemical kinetics. For example, hydroxyl concentrations in turbulent jet flames achieve maximum values several times larger than those predicted by chemical equilibrium low in the flames and decay with increasing height owing to the relatively slow three-body recombination reactions responsible for OH destruction.[7] For this case the change in OH concentration through the jet represents much more than a simple mixing process. On the other hand, some reactive scalars, including OH, display strong correlations with the local mixture fraction despite their departure from a simple laminar flamelet description.[7] Thus, at a given location, instantaneous OH fluctuations may exhibit a strong dependence on the instantaneous mixture fraction fluctuations.

In the present investigation recently compiled OH data are examined for self-similarity with respect to relevant two-time statistics. The time-series measurements of OH concentrations were made by Renfro et al.[8] via a gated-photon counting technique, termed picosecond time-resolved laser-induced fluorescence (PITLIF). All data were obtained in a 78% H_2/22% Ar (by volume) turbulent jet flame in still air. The flame was stabilized on a straight tube burner with an exit diameter of 5.5 mm with no coflow. The laser and detection system provided a spatial resolution of less than 100 μm in all three directions. Time-series measurements of OH were made at 3–5 radial locations across the OH peak at axial locations of $x/D = 1$, 2, 5, 10, and 20 for Reynolds numbers of $Re = 2.8 \times 10^3$, 5×10^3, 9×10^3, 1.3×10^4, and 1.7×10^4, based on the cold-flow average velocity at the jet exit.

Nearly identical flames have been studied experimentally by several other groups.[7,9–11] For example, simultaneous OH concentration and mixture fraction measurements were reported for the same fuel (5.2-mm burner) by Barlow et al.[7] at Reynolds numbers of 8.5×10^3 and 1.7×10^4. These single-shot measurements permitted determination of probability density functions (PDFs). Employing the same fuel, Chen and Mansour[11] obtained simultaneous, multipoint OH concentration and mixture fraction measurements, thus allowing examination of radial scalar dissipation rates in a 4.8-mm jet at Reynolds numbers of 8.8×10^3 and 1.76×10^4. Many experiments in other hydrogen jet flames have also examined hydroxyl concentrations. However, the measurements of Renfro et al.[8] provide the only data that permit investigation of timescales for hydroxyl concentration fluctuations.

In the following section a suitable correction is derived to account for the effects of shot noise in PITLIF measurements of the autocorrelation function. From the resulting quantitative correlations the hydroxyl integral timescales are computed. Normalization using these scales is shown to collapse the measured temporal correlations for OH throughout each of the flames studied. This result implies that a single timescale is sufficient to describe the measured OH fluctuations, which is unexpected for reactive scalars owing to the uncertain impact of those scalar fluctuations related to chemical production and destruction. Finally, the evolution of the measured OH integral timescales is examined for the present reacting jets and compared to predictions of timescales for mixture fraction fluctuations in both reacting and nonreacting jets.

Data Reduction

Significant complications arise when attempting time-series measurements of minor-species concentrations. The details concerning

Received 15 May 1999; revision received 29 September 1999; accepted for publication 11 October 1999.

*Research Assistant, School of Mechanical Engineering.
†Professor, School of Mechanical Engineering. Member AIAA.
‡Associate Professor, School of Mechanical Engineering.
§Reilly Professor of Combustion Engineering, School of Mechanical Engineering.

the measurement technique and the procedures by which it is made quantitative are fully discussed by Renfro et al.[8] At each measurement location in the flames investigated, 50 separate time series of 4000 samples were taken at a sampling rate of 4000 Hz. Renfro et al.[8] present PSDs and PDFs computed from these times series. In addition to these statistics, the present investigation makes use of the autocorrelation function.

The autocorrelation function ρ and the PSD are formally defined by[12]

$$\rho_m(\Delta t) = \frac{\overline{[\mathrm{OH}]'(t)[\mathrm{OH}]'(t+\Delta t)}}{([\mathrm{OH}]'_{\mathrm{rms}})^2} \tag{1}$$

$$\mathrm{PSD}_m(f) = \frac{|\Im\{[\mathrm{OH}]'(t)\}|^2}{([\mathrm{OH}]'_{\mathrm{rms}})^2} = \Im\{\rho_m(\Delta t)\} \tag{2}$$

where $[\mathrm{OH}]' = [\mathrm{OH}] - \overline{[\mathrm{OH}]}$ is the fluctuating part of the time series $[\mathrm{OH}]'_{\mathrm{rms}} = \sqrt{[\mathrm{OH}]'^2}$ and $\Im$ represents a Fourier transform. Both Eqs. (1) and (2) are strictly defined for an infinite amount of continuous data. Because the measured OH time series represents a finite amount of discrete data, a working definition for the autocorrelation function must be used, i.e.,[12]

$$\rho_m(\Delta t_i) = \frac{\sum_{j=0}^{N-i}[\mathrm{OH}]'_j[\mathrm{OH}]'_{j+i}}{\sum_{j=0}^{N}([\mathrm{OH}]'_j)^2} \tag{3}$$

where the discrete time series of N hydroxyl concentration measurements is represented by $[\mathrm{OH}]_j$ for the jth sample time t_j.

The subscript m in Eqs. (1–3) indicates that these are computed directly from the measurements. However, in our measured time series, signal fluctuations occur from both real hydroxyl concentration fluctuations and from shot noise in the photon counting system. The autocorrelation function is affected by both fluctuation sources. Fortunately, Gaskey et al.[13] have found that, because shot-noise fluctuations are uncorrelated with concentration fluctuations, any measured power spectrum is a weighted sum of the contributions from both fluctuation sources considered separately. Furthermore, the shot-noise fluctuations are uncorrelated with themselves so that the shot-noise PSD is uniform over all frequencies. Thus, a shot-noise corrected PSD can be computed from the measured PSD by[8]

$$\mathrm{PSD}_{\mathrm{OH}}(f) = \frac{\mathrm{PSD}_m(f) - C^2|\ f_c}{1 - C^2} \tag{4}$$

where $C = \sigma_{\mathrm{SN}}/\sigma$ is the shot-noise fluctuation intensity normalized by the total fluctuation intensity (rms) and f_c is the high-frequency cutoff in the PSD, which is equal to half the sampling rate. The fraction C can be found by averaging the PSD at high frequencies where shot noise is dominant.[8] The preceding PSD correction was found to work well for the present OH measurements by Renfro et al.[8] Because the autocorrelation function is the inverse Fourier transform of the PSD, the shot-noise corrected autocorrelation function becomes

$$\rho_{[\mathrm{OH}]}(\Delta t_i) = \frac{\Im^{-1}\{\mathrm{PSD}_m(f)\}}{1 - C^2} - \frac{C^2}{(1 - C^2)}\Im^{-1}\left\{\frac{1}{f_c}\right\}$$

$$= \frac{\rho_m(\Delta t_i)}{1 - C^2} - \frac{C^2}{1 - C^2}\delta_{\Delta t_i, 0} \tag{5}$$

Equation (5) shows that the autocorrelation function for the shot-noise contribution is a delta function at zero. This feature is expected because shot noise is uncorrelated for all nonzero time delays. The factor f_c in the second Fourier transform is a result of the data being discrete, i.e., the delta function is finite in width.

Figure 1a shows the autocorrelation functions for OH fluorescence and concentration as measured in the $Re = 9 \times 10^3$ flame at $x/D = 20$, 2 mm to the fuel side of the maximum [OH]. As determined from the PSDs, the shot-noise factor is $C = 0.30$ for the fluorescence measurement and $C = 0.81$ for the concentration measurement at this location. As discussed by Renfro et al.,[8] the effects of shot noise are worse for concentration, which must be corrected for fluorescence lifetime variations, as compared to the fluorescence

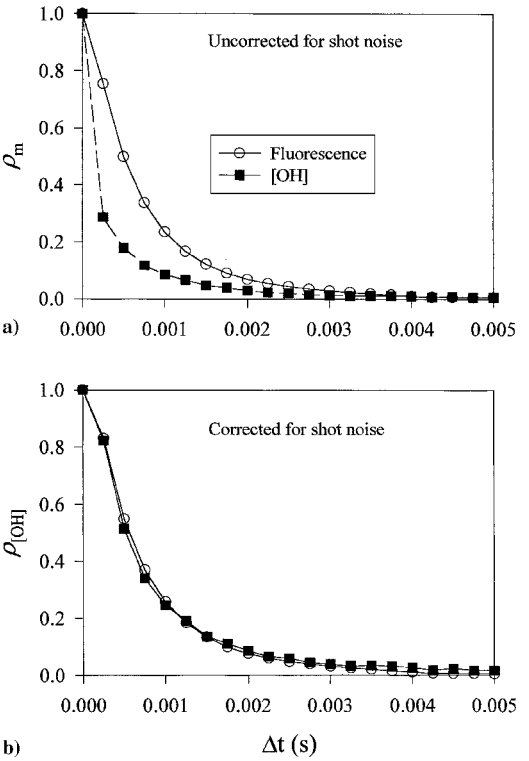

Fig. 1 Hydroxyl concentration and fluorescence autocorrelation functions measured 2 mm to the fuel side of the [OH] peak at $x/D = 20$ in the $Re = 9 \times 10^3$ flame. The shot-noise corrected autocorrelation functions ($\rho_{[\mathrm{OH}]}$) are computed from the measured functions (ρ_m) via Eq. (5).

signal, which is directly measured. The uncorrected concentration correlation (ρ_m) drops off much faster than that for fluorescence owing to the shot-noise delta function at zero. Without correcting for shot noise, the correlation functions for concentration and fluorescence differ. In comparison, Fig. 1b shows the autocorrelation functions for concentration and fluorescence after correction for shot noise ($\rho_{[\mathrm{OH}]}$). These are nearly identical, consistent with the PSDs already reported.

The accuracy of the noise correction is affected by both the measurement of C^2 and the signal-to-noise ratio. For each of the measurements reported here, C^2 is determined with an uncertainty of only ±4% (95% confidence interval)[8] owing to the large amount of data (50 independent series) collected at each location. The signal-to-noise ratio (SNR) for both the PSD and autocorrelation function is simply the ratio of the intensity of fluctuations arising from concentration to those arising from shot noise. From rearrangement of Eq. (4), the SNR is found to be equal to $1/C^2 - 1$. For each of the present measurements, the SNR is always greater than 3 and is often as large as 20.

In the next section the integral timescale τ_I for these measurements is examined. The integral timescale represents approximately the largest time over which fluctuations are correlated and is defined by

$$\tau_I = \int_0^\infty \rho_{[\mathrm{OH}]}(\Delta t)\,\mathrm{d}\Delta t \tag{6}$$

As for the autocorrelation function, Eq. (6) is defined for an infinite and continuous time record; thus, τ_I can only be estimated from the discrete autocorrelation function by using a numerical integration. However, for the relatively long time series considered here, the discrete representation for τ_I is close to that defined in Eq. (6).[12] Without correcting for shot noise, the measured integral timescales will be systematically reduced by a factor of roughly $1 - C^2$. The impact of this correction can be observed by comparing Figs. 1a and 1b for which the areas under the concentration autocorrelation functions are notably different. Hence, the preceding shot-noise correction has been applied to each of the statistics reported in the remainder of this paper.

Renfro et al.[8] have also used this shot-noise correction to determine relative [OH] rms values with an uncertainty of ±10% (95% confidence interval). The relative $[OH]_{rms}$ values are normalized by the mean [OH] values, which have a ±18.5% uncertainty (95% confidence interval) arising from the fluorescence calibration procedure.[8] We have further examined the accuracy of this noise correction by repeating the integral timescale measurements nine times over seven days, each with a different level of noise. The uncertainty in the integral timescale was found to be ±22.2% (95% confidence interval).

Results

Figure 2a shows the autocorrelation function for each flame at the radial location of peak [OH] for $x/D = 5$, 10, and 20. The exact location for each of these measurements is tabulated by Renfro et al.[8] The integral timescale decreases significantly with increasing Reynolds number. As a result, the autocorrelation functions show significant variations in width. However, Fig. 2b shows the same data normalized by the measured integral timescale. The normalized autocorrelation function is the same for each measurement, independent of the Reynolds number and axial height. The autocorrelation functions for $x/D < 20$ in the $Re = 2.8 \times 10^3$ flame are not shown in Fig. 2. At these locations significant periodic fluctuations are present, similar to those reported previously in the near field of diffusion flames.[14] These fluctuations manifest themselves as a strong frequency in the PSD[8] and equivalently as a sinusoid in the autocorrelation trace. These PSDs do not collapse with the others, but this behavior is, of course, not unexpected as the statistics for large-scale oscillations are not represented by a purely turbulent autocorrelation function.

When autocorrelation functions for $x/D = 1$ and 2 are considered in addition to those in Fig. 2, the collapse is still observed, but significantly more scatter is present. For example, Fig. 3a shows OH concentration autocorrelation functions for three radial locations at each axial height in the $Re = 9 \times 10^3$ flame. Near the burner exit the autocorrelation functions show considerable correlation for large time delays (large-scale, low-frequency fluctuations). Nevertheless, for small time delays (small-scale, high-frequency fluctuations), the

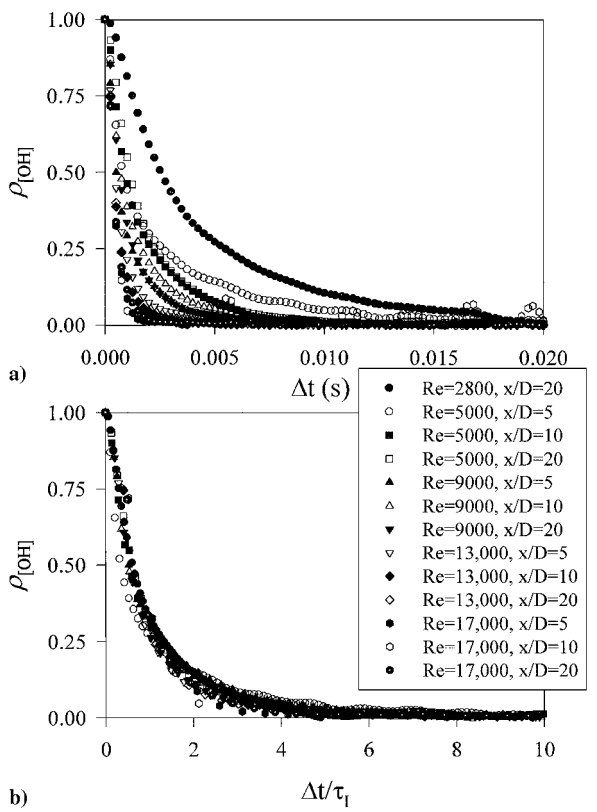

Fig. 2 Autocorrelation functions for [OH] at the radial location of peak OH concentration in each flame.

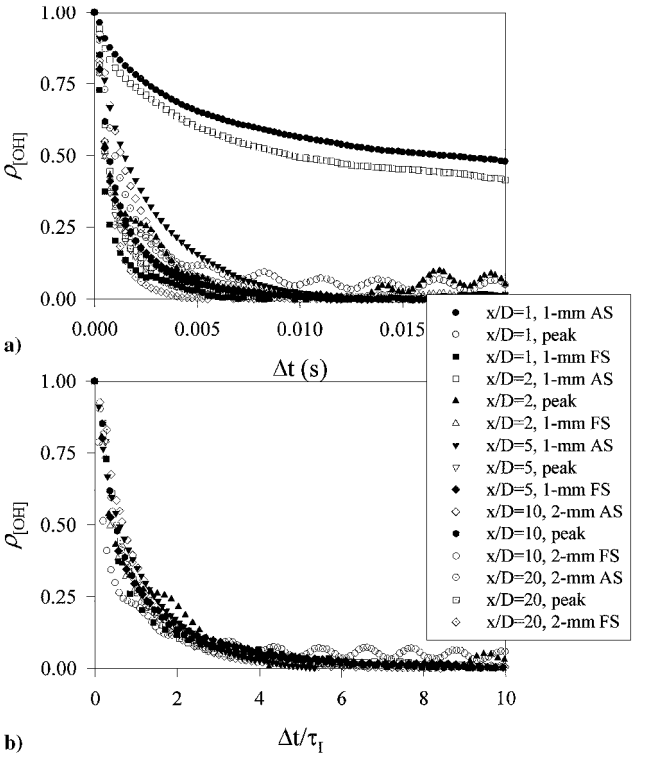

Fig. 3 Autocorrelation functions for [OH] in the $Re = 9 \times 10^3$ flame. Measurements are reported for the radial location of peak [OH] and for locations relative to the peak on both the air side (AS) and the fuel side (FS).

autocorrelation functions for $x/D = 1$ and 2 are quite close to those for the downstream locations. However, the measurements toward the air side of the peak concentrations at $x/D = 1$ and 2 show integral timescales significantly larger than any of the other measurements. At these low heights the hydroxyl peaks are located outside of the turbulent flow and may undergo significant laminarization.[15,16] Hence, these autocorrelation functions are more representative of a laminar flow for which all time delays are perfectly correlated. Figure 3b shows the scaled autocorrelation functions. The two near-laminar measurement locations are not shown in Fig. 3b as they do not collapse with the remaining measurements. It may be possible to account for laminar flow effects by including an intermittency parameter, but this is beyond the scope of the present investigation.

The scatter in the normalized autocorrelation functions in Fig. 3b is worse than that in Fig. 2b. Several measurement locations (e.g., the peak [OH] location at $x/D = 1$ and 2) display a noticeable sinusoidal fluctuation in the autocorrelation function. This is indicative of a single-frequency oscillation, as with buoyancy; however, these fluctuations are at ~360 Hz, which is far too large to be a buoyancy-induced oscillation.[17] The PSDs from these locations also show a strong component at ~360 Hz (e.g., Renfro et al.,[8] Fig. 7); however, the width of this peak in the PSD is very narrow so that the intensity of the [OH] fluctuations resulting from this oscillation is quite small. Hence, this feature is likely either a noise artifact or a large-scale periodic fluctuation,[14] which is apparent at these locations because of the reduced [OH] fluctuations. Away from the peak concentration and further downstream, the OH concentration fluctuations are several times larger than those at the peak concentration at $x/D = 1$ and 2 (Ref. 8), such that this small artifact is no longer visible.

An autocorrelation function can be computed free of the 360-Hz oscillation by taking the inverse Fourier transform of the PSD with the value at 360 Hz set equal to the average of that at 359 and 361 Hz. For the measurements at $x/D = 1$, this procedure still does not cause the autocorrelation functions to collapse as $\rho_{[OH]}$ is significantly above zero for large time delays. Thus, the larger scatter observed for the normalized autocorrelation functions of Fig. 3b appears to be a result of both small single-frequency components and the location of the OH layer in a laminar regime at these heights.[16] Figure 4 shows the same autocorrelation functions as Fig. 3 except

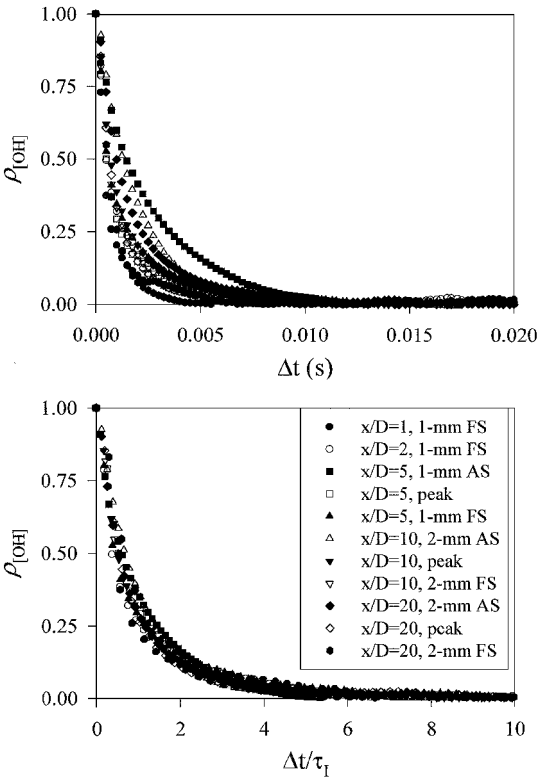

Fig. 4 Same data as Fig. 3 without air side and peak measurements at $x/D = 1$ and 2.

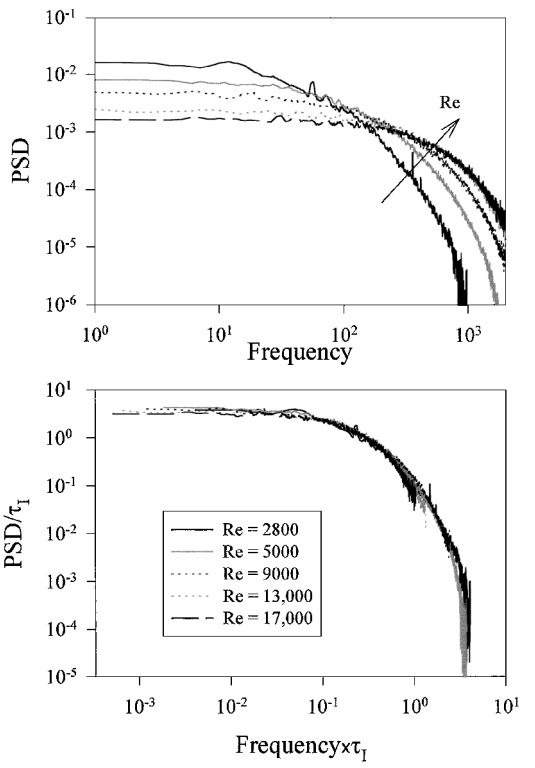

Fig. 5 Power spectral densities measured at the location of peak [OH] at $x/D = 20$ in each flame. Integral timescales used to normalized the PSDs were computed from the autocorrelation functions of Fig. 2.

with the air side and peak data removed at $x/D = 1$ and 2. The collapse of all remaining measurements is observed to be equivalent to that in Fig. 2. Hence, the autocorrelation function shape is independent of Reynolds number, axial height, and radial location in these jet flames for all locations except those very low in the flames where the OH profile resides outside of the turbulent flow. This result is remarkable because the Dahmköhler number varies by two orders of magnitude over the conditions $x/D = 5$–20 and $Re = 2.8 \times 10^3$–1.7×10^4 (Ref. 7). Thus, whereas the relative timescale for chemical reactions changes significantly, the normalized autocorrelation function remains the same.

Because the PSD and autocorrelation function are Fourier transform pairs, a similar collapse of the measured PSDs is expected when scaled by the integral timescale. This collapse is shown in Fig. 5 for measurements at the [OH] peak for $x/D = 20$ in each flame. The same integral timescales as computed from Fig. 2 are effective in collapsing the PSDs. Because each measurement was taken at a sampling rate of 4 kHz, the highest dimensional frequency resolved in the PSDs is 2 kHz. However, the integral timescale decreases as the Reynolds number rises such that the measurements in the higher-Reynolds-number flames resolve lower nondimensional frequencies.

The increased frequency of the OH fluctuations at higher Reynolds numbers can also be discerned directly from the measured time series. Figure 6 shows 0.1 s of OH data from the $Re = 2.8 \times 10^3$, 9×10^3, and 1.7×10^4 measurements used to compile Fig. 5. These time series were selected randomly and are typical of the full 50 s of data collected at each location. Each of these time series has been normalized by the appropriate mean [OH] values, which are tabulated by Renfro et al.[8] All three time series in Fig. 6 display a similar range of values about the mean despite the large change in fluctuation timescales.

Because the frequencies of the OH fluctuations increase at higher Reynolds numbers, the sampling rate should obviously be increased as the Reynolds number rises. Unfortunately, this is only possible up to the point at which shot-noise fluctuations become dominant. For each of the measurements reported here, the PSD begins to flatten at high frequencies as a result of shot noise (e.g., Renfro et al.,[8] Fig. 3). It is unlikely that higher frequencies can be directly

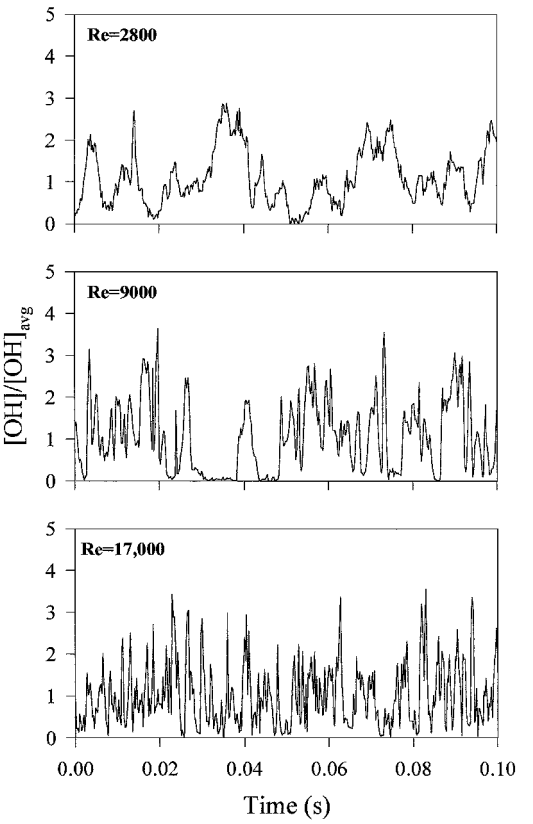

Fig. 6 Sample time series measured at the peak [OH] location for $x/D = 20$ in the $Re = 2.8 \times 10^3$, 9×10^3, and 1.7×10^4 flames. These time series represent the first 0.1 s of data collected at each location and are representative of the full 50 s.

resolved in these flames without a significant increase in signal, say by improved laser technology or by reduced spatial resolution. On the other hand, the good collapse of the measured autocorrelation functions and PSDs in these flames suggest that the measurements at lower Reynolds numbers can be extended to the flames at higher Reynolds numbers. In other words, because the dimensionless $Re = 1.7 \times 10^4$ PSD matches that at lower Reynolds numbers up to a frequency of $\sim 1/\tau_I$, the low-Reynolds-number PSD could be assumed to be valid up to higher frequencies, effectively increasing the temporal resolution of the $Re = 1.7 \times 10^4$ PSD. However, this approach can cause problems because use of the integral timescale for collapse of the PSDs does not consider the separation between τ_I and the Kolmogorov timescale (or Batchelor timescale for scalars) as a function of Reynolds number.[4] In other words, the normalized spectrum that appears to describe adequately each of the PSDs of Fig. 5 is valid only up to timescales for which dissipation becomes significant, and this will occur at different normalized frequencies for each Reynolds number.[5]

In summary, each measured OH time series for $x/D = 5$–20 and $Re = 2.8 \times 10^3$–1.7×10^4 is observed to collapse onto the same normalized autocorrelation function, or equivalently PSD, at least up to the frequencies resolved by these measurements. These nondimensional curves are shown in Fig. 7a for the autocorrelation function and Fig. 7b for the PSD. Also shown for comparison is an exponential autocorrelation function and its power spectral density. Mixture fraction fluctuations in both nonreacting jets[3] and jet diffusion flames[6] have been found to be closely approximated by an exponential autocorrelation function. The agreement here is very similar to that noted by Kounalakis et al.[6] for mixture-fraction measurements in turbulent CO/H_2 flames. In particular, the exponential function is adequate for low frequencies (large time delays) and captures the general shape of the PSD. However, the exponential autocorrelation function does not capture the correct curvature near $\Delta t = 0$, where the first derivative should be zero because the autocorrelation function is even and infinitely differentiable.[4] Thus, for very small time delays the exponential decays too quickly as compared to the measured [OH] correlation. At intermediate time delays ($0.5\tau_I < \Delta t < 2.0\tau_I$) all of the measured data are less correlated than predicted by an exponential decay. Both of these observations are consistent with the mixture fraction correlations of Kounalakis et al.[6]

For the PSD the measured data decay with a much steeper slope than that predicted by the exponential autocorrelation function at large frequencies. On the other hand, the data available for $f > 1/\tau_I$ are limited to the two lowest Reynolds-number flames. This steepening of the power spectra could be a result of the effects of dissipation near the Batchelor scale. As just mentioned, use of the integral timescale for collapse of the PSDs should not extend to the dissipation range of the spectra.

Having demonstrated the effectiveness of the integral timescale in collapsing the measured autocorrelation functions and PSDs at low to moderate frequencies, we now examine the evolution of τ_I as a function of Re, x, and r in these flames. The integral timescale is proportional to some relevant length scale divided by some relevant velocity scale. Taking the local velocity and jet width as the appropriate scales, the velocity integral timescale would be expected to follow

$$\tau_I \sim \frac{L}{U(x,r)} \sim \left(\frac{1}{U_e}\right)\left(\frac{LU_e}{U_{cl}(x)}\right)\left(\frac{U_{cl}(x)}{U(x,r)}\right) \sim \left(\frac{1}{Re}\right)\left(\frac{x}{D}\right)^2 f\left(\frac{r}{x}\right) \tag{7}$$

where L is the integral length scale, which grows linearly with axial distance,[4] $U(x,r)$ is the local velocity, U_e is the average velocity at the burner exit ($\sim Re$), $U_{cl}(x)$ is the centerline velocity ($\sim U_e/x$), and $f(r/x)$ is some function of the normalized radial coordinate. This scaling procedure is also discussed by Magre and Dibble.[10] For nonreacting jets, where the mixture fraction develops similar to velocity, the integral timescale for mixture fraction should also scale as in Eq. (7). This scaling has indeed been observed.[3,18] Figure 8 shows τ_I for OH fluctuations at $x/D = 20$ in each flame (as a function of only Reynolds number). Somewhat surprisingly, the hydroxyl timescales have the same linear dependence on $1/Re$ as the velocity and mixture fraction timescales.

Unfortunately, the OH profile does not reside at the same radial location (r/x) at all axial heights, particularly low in these flames.[8] Thus, the axial scaling of Eq. (7) cannot be simply separated from any radial dependence of τ_I as reflected by $f(r/x)$. Figure 9 shows all of the integral timescales of this study scaled for Reynolds number and axial location (assuming $\tau_I \sim x^2$) as a function of relative radial location (r/x). The collapse of τ_I to nearly a single curve indicates that the assumed axial scaling is reasonably valid. On the other hand, there is over a four order-of-magnitude variation in these normalized timescales, and the comparison in log coordinates does not provide a sensitive measure of the exact axial variation, i.e., an assumed dependence of $x^{1.75}$ to $x^{2.25}$ would visually look just as good.

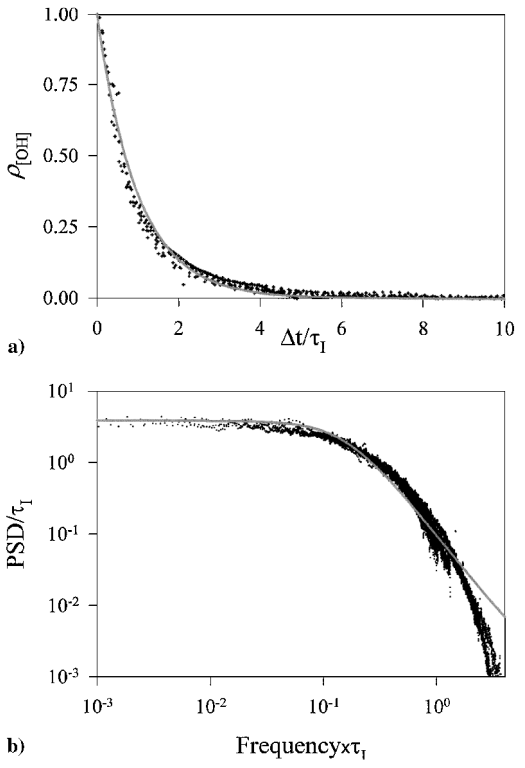

Fig. 7 Comparison of collapsed statistics with those of an exponential autocorrelation function. The individual data points represent each of the measurements from Figs. 2, 4, and 5.

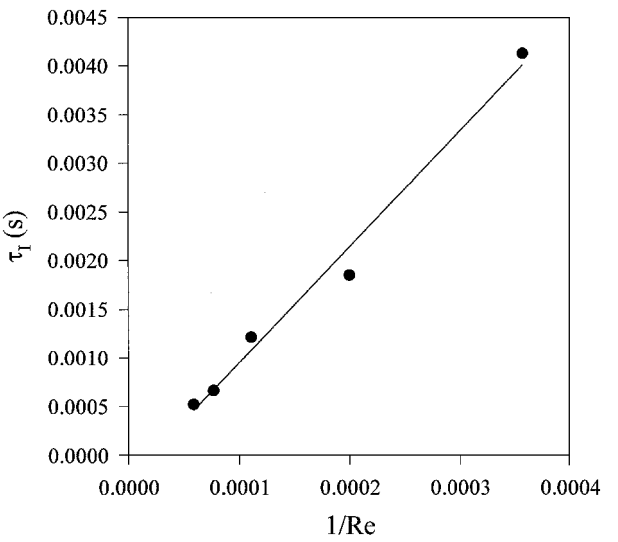

Fig. 8 Integral timescales computed from the autocorrelation functions of Fig. 2 for the locations of peak [OH] at $x/D = 20$ in each flame.

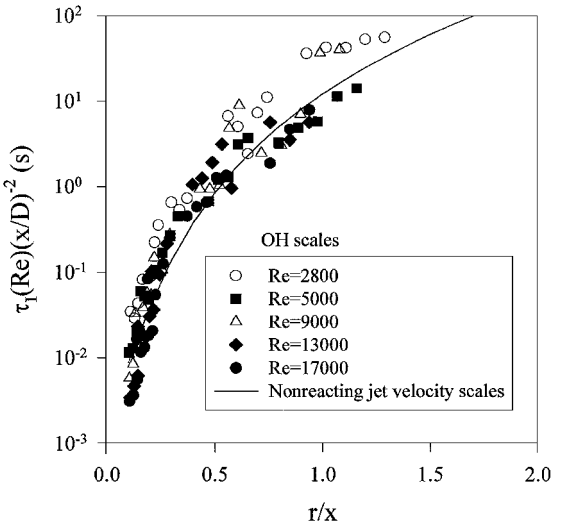

Fig. 9 Normalized integral timescale computed for every time series of the present flames. The expected integral timescales based on the nonreacting-jet velocity correlation of Schlichting[19] are also shown.

Similarly, Kounalakis et al.[6] find that their mixture-fraction integral timescales collapse when normalized by only x. These authors provide data for only a few axial locations (as with our measurements) and use a virtual origin in their normalization such that the sensitivity of the collapse to the exponent of x^n is also weak. For nonreacting jets a scaling of x^2 for mixture fraction appears to be correct,[3,18] but improved measurements of mixture fraction in reacting jets are needed to resolve this scaling issue in turbulent flames.

Figure 9 also shows a comparison of the measured timescales with those predicted based on a self-similar radial profile for velocity in nonreacting jets.[19] Once again, the OH timescales appear to reasonably follow temporal statistics that are similar to those for velocity in nonreacting jets.

Discussion

The self-similarity of OH PSDs for flames with Reynolds numbers as low as 2.8×10^3 is somewhat surprising in view of previous work.[15,16] Seitzman et al.[15] measured OH spatial distributions in hydrogen jet flames at $x/D = 2.5$–40 and found that OH exists in a nearly laminar layer at $Re = 2.3 \times 10^3$. Likewise, Clemens and Paul[16] measured the OH structure in the near field ($x/D < 2.5$) of hydrogen/nitrogen flames and found completely laminarized thin OH layers that were not perturbed by the fuel-stream turbulence. However, in pure hydrogen flames, Clemens and Paul[16] found that the OH distribution was thin below $x/D = 2.5$ but slightly perturbed by the fuel stream as a result of the lower fuel density. At higher Reynolds numbers and further downstream ($x/D = 2.5$–40), Seitzman et al.[15] showed that the structure of the OH distribution changes from thin filaments to both thin and diffuse distributions. However, these higher-Reynolds-number flames were lifted, and it is likely that their OH structure is inherently different than for attached flames. For all of our hydrogen/argon flames, with a fuel density between the hydrogen and hydrogen/nitrogen cases of Clemens and Paul,[16] it is likely that OH exists in only a thin region.

The discrepancy that we see in our autocorrelation functions at $x/D < 5$ is probably a result of the laminarized near-field behavior of these turbulent diffusion flames.[16] Nevertheless, farther downstream, the perturbations of the thin OH layer caused by fuel-stream turbulence are apparently sufficient to be measured by the time-series technique and to yield a turbulence spectrum. At $Re = 70$ the PITLIF technique gives flat PSDs[20] arising from purely laminar flows. Hence, the unexpected collapse of the $Re = 2.8 \times 10^3$ case at $x/D = 20$ is not a measurement artifact, but is most likely a result of thin OH flamelets that exist over the entire range from $Re = 2.8 \times 10^3$ to 1.7×10^4. An additional complication is that our flames are significantly affected by buoyancy,[21] which can increase the momentum flux at downstream locations for lower Reynolds numbers and may thus contribute to the collapse of the time-series statistics. Thus, the interpretation of our results is presently limited to moderate Reynolds numbers. Whether the observed self-similarity will hold for higher-Reynolds-number flames and for higher frequencies than those resolved in the present experiments are interesting questions for future work.

Nevertheless, for the range $Re = 2.8 \times 10^3$–1.7×10^4, which is common to many laboratory experiments and practical flows, the self-similarity of OH temporal statistics at sufficiently high x/D is certainly intriguing. Transient models of turbulent combustion can be evaluated effectively based on their ability to predict such results. In addition, the measured hydroxyl fluctuations are found to follow approximately an exponential autocorrelation function. However, the present measurements were limited to a sampling frequency of 4 kHz. For larger frequencies for which dissipation is significant, the autocorrelation functions should not collapse when scaled by the integral timescale.

Because local OH fluctuations in these flames appear to follow the same temporal statistics as local mixture fraction fluctuations, a simple one-dimensional laminar flamelet approach to modeling of OH PSDs may yield good agreement with measurements.[22] On the other hand, peak OH concentrations as a function of axial height in similar flames have been shown to depend strongly on the Dahmköhler number owing to the existence of superequilibrium OH concentrations,[7] which also affects the flame temperature.[10] Thus, matching the measured variation in peak OH concentration via flamelet modeling may require different state relationships for each height (or perhaps two-dimensional state relationships).

This apparent discrepancy arises because the collapse of the temporal statistics does not require a collapse of the associated PDFs, which display various shapes in different regions of the present flames.[8] Renfro et al.[22] simulated minor-species PSDs for these flames using laminar flamelet state relationships and found that the simulations were sensitive to the mixture fraction statistics and concentration profile width, but were fairly insensitive to the exact profile shape and peak concentration. In contrast, the PDF depends strongly on the profile shape and the peak concentration. PDFs and PSDs describe separate information about the scalar fluctuations. Although these statistics are computed from the same time series, it appears that they are nearly independent of one another. We are presently investigating means of incorporating realistic PDF and PSD behavior into mixture fraction time-series simulations so that critical comparisons can be made between predictions of different combustion models, including the laminar flamelet model.

Conclusions

Recent hydroxyl time-series measurements obtained by Renfro et al.[8] have been examined for statistical similarity with respect to autocorrelation functions and PSDs. By normalizing these two-time statistics by the measured OH integral timescale, a single normalized autocorrelation function (and PSD) was found to describe all of the data in the investigated flames for $Re = 2.8 \times 10^3$–1.7×10^4 and $x/D = 5$–20. The collapse of the measured statistics for measurements at $x/D = 1$ and 2 is worse than for measurements further downstream. At these lower heights, measurements made toward the ambient air side were found to display large variations, most probably as a result of the nearly laminar flow in these regions.

The observed collapse of the autocorrelation functions demonstrates that hydroxyl fluctuations are adequately described by a single timescale and thus a single normalized autocorrelation function. This is not an expected result for reactive scalars because both turbulent mixing and chemical reaction can affect [OH] fluctuations, and the timescales for these two processes are not the same. Moreover, multiple chemical timescales exist for species such as OH so that Dahmköhler numbers both greater than and less than unity are present in these flames.[7]

Acknowledgments

This research was supported by the U.S. Air Force Office of Scientific Research, with Julian Tishkoff serving as technical monitor, and by a Department of Defense fellowship. We appreciate the very helpful comments made by one reviewer of the original manuscript.

References

[1]Hussein, J. H., Capp, S. P., and George, W. K., "Velocity Measurements in a High-Reynolds-Number, Momentum-Conserving, Axisymmetric, Turbulent Jet," *Journal of Fluid Mechanics*, Vol. 258, 1994, pp. 31–75.

[2]Wygnanski, I., and Fiedler, H., "Some Measurements in the Self-Preserving Jet," *Journal of Fluid Mechanics*, Vol. 38, Pt. 3, 1969, pp. 577–612.

[3]Birch, A. D., Brown, D. R., Dodson, M. G., and Thomas, J. R., "The Turbulent Concentration Field of a Methane Jet," *Journal of Fluid Mechanics*, Vol. 88, Pt. 3, 1978, pp. 431–449.

[4]Tennekes, H., and Lumley, J. L., *A First Course in Turbulence*, MIT Press, Cambridge, MA, 1972.

[5]Uberoi, M. S., and Freymuth, P., "Spectra of Turbulence in Wakes Behind Circular Cylinders," *Physics of Fluids*, Vol. 12, No. 7, 1969, pp. 1359–1363.

[6]Kounalakis, M. E., Sivathanu, Y. R., and Faeth, G. M., "Infrared Radiation Statistics of Nonluminous Turbulent Diffusion Flames," *Journal of Heat Transfer*, Vol. 113, May 1991, pp. 437–445.

[7]Barlow, R. S., Dibble, R. W., Chen, J.-Y., and Lucht, R. P., "Effect of Damköhler Number on Superequilibrium OH Concentration in Turbulent Nonpremixed Jet Flames," *Combustion and Flame*, Vol. 82, 1990, pp. 235–251.

[8]Renfro, M. W., King, G. B., and Laurendeau, N. M., "Quantitative Hydroxyl-Concentration Time-Series Measurements in Turbulent Nonpremixed Flames," *Applied Optics*, Vol. 38, No. 21, 1999, pp. 4596–4608.

[9]Driscoll, J. F., Schefer, R. W., and Dibble, R. W., "Mass Fluxes $\overline{\rho' u'}$ and $\overline{\rho' v'}$ Measured in a Turbulent Nonpremixed Flame," *Nineteenth Symposium (International) on Combustion*, Combustion Inst., Pittsburgh, PA, 1982, pp. 477–485.

[10]Magre, P., and Dibble, R., "Finite Chemical Kinetics Effects in a Subsonic Turbulent Hydrogen Flame," *Combustion and Flame*, Vol. 73, 1988, pp. 195–206.

[11]Chen, Y.-C., and Mansour, M. S., "Measurements of the Detailed Flame Structure in Turbulent H_2-Ar Jet Diffusion Flames with Line-Raman/Rayleigh/LIPF-OH Technique," *Twenty-Sixth Symposium (International) on Combustion*, Combustion Inst., Pittsburgh, PA, 1996, pp. 97–103.

[12]Box, G. E. P., Jenkins, G. M., and Reinsel, G. C., *Time Series Analysis*, 3rd ed., Prentice–Hall, Upper Saddle River, NJ, 1994.

[13]Gaskey, S., Vacus, P., David, R., Villermaux, J., and André, J. C., "A Method for the Study of Turbulent Mixing Using Fluorescence Spectroscopy," *Experiments in Fluids*, Vol. 9, 1990, pp. 137–147.

[14]Savas, Ö., and Gollahalli, S. R., "Flow Structures in Near-Nozzle Region of Gas Jet Flames," *AIAA Journal*, Vol. 24, 1986, pp. 1137–1140.

[15]Seitzman, J. M., Üngüt, A., Paul, P. H., and Hanson, R. K., "Imaging and Characterization of OH Structure in a Turbulent Nonpremixed Flame," *Twenty-Third Symposium (International) on Combustion*, Combustion Inst., Pittsburgh, PA, 1990, pp. 637–644.

[16]Clemens, N. T., and Paul, P. H., "Effects of Heat Release on the Near Field Flow Structure of Hydrogen Jet Diffusion Flames," *Combustion and Flame*, Vol. 102, 1995, pp. 271–284.

[17]Chen, L.-D., Seaba, J. P., Roquemore, W. M., and Goss, L. P., "Buoyant Diffusion Flames," *Twenty-Second Symposium (International) on Combustion*, Combustion Inst., Pittsburgh, PA, 1988, pp. 677–684.

[18]Becker, H. A., Hottel, H. C., and Williams, G. C., "The Nozzle-Fluid Concentration Field of the Round, Turbulent, Free Jet," *Journal of Fluid Mechanics*, Vol. 30, Pt. 2, 1967, pp. 285–303.

[19]Schlichting, H., *Boundary-Layer Theory*, McGraw–Hill, New York, 1979, pp. 747–750.

[20]Renfro, M. W., Pack, S. D., King, G. B., and Laurendeau, N. M., "Hydroxyl Time-Series Measurements in Laminar and Moderately Turbulent Methane/Air Diffusion Flames," *Combustion and Flame*, Vol. 115, 1998, pp. 443–455.

[21]Becker, H. A., and Yamazaki, S., "Entrainment, Momentum Flux and Temperature in Vertical Free Turbulent Diffusion Flames," *Combustion and Flame*, Vol. 33, 1978, pp. 123–149.

[22]Renfro, M. W., Sivathanu, Y. R., Gore, J. P., King, G. B., and Laurendeau, N. M., "Time-Series Analysis and Measurements of Intermediate Species Concentration Spectra in Turbulent Nonpremixed Flames," *Twenty-Seventh Symposium (International) on Combustion*, Combustion Inst., Pittsburgh, PA, 1998, pp. 1015–1022.

R. P. Lucht
Associate Editor